Population-based Approach to Estimate Corrosion Growth in Pipelines

Markus R. Dann
Assistant Professor, Department of Civil Engineering, University of Calgary, Calgary, Canada

Marc A. Maes
Professor, Department of Civil Engineering, University of Calgary, Calgary, Canada

ABSTRACT: Corrosion in pipelines can lead to leak and rupture failures with significant consequences for people, the economy, and the environment. Corrosion growth rates are often determined from the results of in-line inspections. Detected corrosion anomalies from at least two inspections are matched with respect to their location in the pipeline and the measured growth path is used to infer current and future corrosion growth. Reliable defect matching is essential to infer credible corrosion rates for pipeline integrity assessments. If high-density corrosion is present, as frequently observed in upstream and subsea pipelines, reliable matching can typically be performed for a limited number of features. The remaining unmatched elements are usually removed from the corrosion growth analysis. The objective of this paper is to introduce a population-based corrosion growth analysis that neither requires matched defects nor removes corrosion anomalies from the analysis. All reported corrosion anomalies from an inspection are considered as a single population and the probabilistic approach determines the corrosion growth of two given populations. Adjustments are included for sizing, detectability, and false call uncertainties to determine the underlying true corrosion growth process. The results are used to estimate future corrosion evolution in joints and entire pipeline segments for informed deterministic or reliability-based integrity assessments of pipelines. The major advantage of this new approach is that the model can easily process mass pipeline inspection data.

1. INTRODUCTION

Corrosion is a time-dependent process that causes gradual metal loss in pipelines. Failures in pipelines can possibly lead to severe consequences for society, the environment, and the economy. Pipeline integrity management (PIM) often relies on a three step approach to ensure that pipeline operations are safe and reliable and to avoid failures. First, in-line inspections (ILIs) are performed to count and size corrosion anomalies in a pipeline. Second, ILI data are analyzed in a corrosion growth analysis and fitness-for-service (FFS) assessment to determine the remaining lifetime of the pipeline. Third, maintenance and repair actions are executed, if necessary, to extend the service life of the pipeline.

The FFS assessment follows standardized procedures (DNV 2010; ASME 2012) and decides whether a detected corrosion anomaly is acceptable. However, guidance on determining the corrosion growth from ILI data is very limited. There are two approaches for the corrosion growth analysis from ILI data:

1. Detected corrosion defects are matched with respect to their location in the pipeline from at least two ILIs. The observed corrosion growth is used to infer the actual corrosion growth. This approach leads to local and defect-specific corrosion growth estimates.

2. Detected corrosion defects from multiple ILIs of the entire pipeline or a pipeline segment are considered in the corrosion growth analysis. No attempt of matching the defects is undertaken. The result is an overall corrosion growth estimate of the entire set of defects.

Research has been primarily focused on the corrosion growth analysis of matched defects (Maes et al. 2009; Maes et al. 2009; Zhang et al. 2013; Zhang and Zhou 2014). State-of-the-art models often rely on a hierarchical framework (Gelman and Hill 2007; Congdon 2010), a stochastic corrosion growth process with strictly positive increments (e.g. gamma process (van Noortwijk 2009)), and include inspection uncertainties (Maes and Dann 2011), such as depth sizing errors, probability of detection, and false call uncertainties. The effort associated with defect matching can be significant and can lead to misidentification and false pairings, particularly for high-density corrosion.

An alternative method to the corrosion growth analysis of matched defects is a population-based (or segment-based) approach that does not require defect matching. To the author's knowledge, applications of the population-based approach have been very limited to the analysis of mean corrosion growth between ILIs (Dawson and Kariyawasam 2009; Bubenik et al. 2014). No full probabilistic analysis has been attempted and, as a result, the information contained in the ILI data has not been used to its fullest extent.

The objective of this paper is to introduce a comprehensive probabilistic framework for the population-based analysis of ILI corrosion data to support the integrity and risk assessment of pipelines subject to corrosion. Special emphasis is given to inspection uncertainties. Section 2 investigates the ILI measurement uncertainties and develops a hierarchical framework for the subsequent analysis. Sections 3 presents the probabilistic analysis with respect to the defect size and number of defects for an individual ILI. The corrosion growth analysis is developed in Section 4 for two inspections. The entire probabilistic approach is demonstrated in an example on actual ILI data in Section 5 and the final conclusions are presented in Section 6.

2. HIERARCHICAL FRAMEWORK FOR PIPELINE ILI UNCERTAINTIES

Pipeline ILIs are subject to four types of measurement errors that are included in the reported ILI data (Maes and Salama 2008; Maes and Dann 2011). First, the inspection tool (IT) does not detect all existing defects; some corrosion anomalies are ignored by the IT and it reports an intact pipe wall at that location. Second, if the anomalies reported by the IT are true corrosion defects, the actual defect size is subject to considerable sizing errors; the reported defect size differs from the actual defect size. Third, if the IT reports a defect having certain dimensions but the pipe wall is intact and the defect does not exist, this fictitious anomaly is referred to as a false call. Fourth, ITs have a lower depth size threshold so that defects below that tool-specific threshold are reported as non-existing.

The ILI measurement errors and the corresponding number of defects and defect sizes can be arranged in a hierarchical order as shown in Figure 1. Each population or set of defects in Figure 1 is described by a 2-element vector (number of defects in the population; size of all defects in the population) where the elements are treated as random variables. The lower level variables depend on the variables in the upper levels in the hierarchical model. At the top of the hierarchy, the population of actual corrosion defects in a pipeline (n, X), which consists of $n \geq 1$ defects and the size (e.g. depth, length, or width) of all n defects is described by the random variable X. Not all n defects are detected due to detectability errors. Hence, the population of actual defects splits into the populations of detected (D) defects (n|D; X|D) and non-detected (ND) defects (n|ND; X|ND) at level 4 in Figure 1. The population of detected defects is also referred to as the set of true calls TC: (n|TC; X|TC). At level 3 sizing errors are added to the actual size of the true calls: (m|TC; Y|TC). The sum of true calls

subject to sizing errors and the false calls (m|FC; Y|FC) is the population of reportable corrosion defects (m; Y). Based on the IT-specific reporting threshold, the population of reportable defects splits into the populations of reported defects (m|R; Y|R) and non-reported defects (m|NR; Y|NR) located at the bottom of the hierarchy (level 1) in Figure 1.

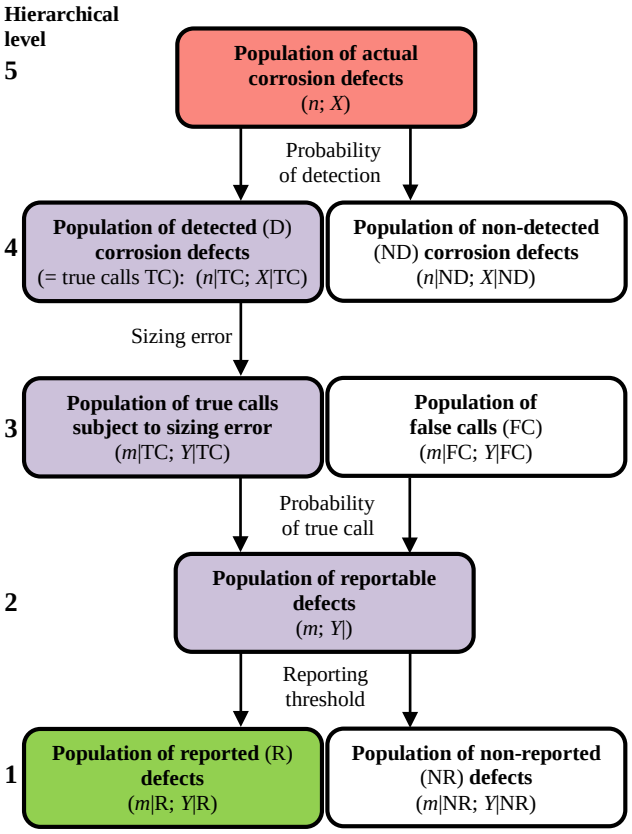

Figure 1: Hierarchical model for a population of corrosion defects subject to ILI uncertainties.

3. ANALYSIS OF THE NUMBER AND SIZE OF CORROSION DEFECTS

The hierarchical model in Figure 1 provides the relationship between the reported defects (m|R; Y|R) that are obtained from the IT and the actual, but unknown, defects in the pipeline (n; X). Pipeline integrity and risk assessments should be based on the actual defect population, which is adjusted for the ILI measurement uncertainties. All quantities in Figure 1 are treated as random variables. The objective of this section is to develop a probabilistic analysis to estimate the number n and the size X of the actual corrosion defects conditional on the reported defect population (m|R; Y|R). A hierarchical Bayes analysis (Dann 2011) is a suitable method to determine the posterior distribution of the unknown random variables; it usually relies on numerical simulation techniques (e.g. Markov Chain Monte Carlo methods (Gamerman and Lopes 2006)), which are implemented in special software tools to obtain samples from the posterior distributions. A step-by-step approach from the bottom to the top level in Figure 1 is used instead of a full hierarchical Bayes approach to determine the distribution of the unknown random variables; this approach allows simple spreadsheet software tools for the population-based ILI data analysis.

Level 1:

The results of an ILI run are the number m|R of reported defects and the measured defect sizes (e.g. depth) y_i|R $\geq$ RT (i = 1 , …, m|R) above the IT-specific reporting threshold RT. The observed defect depths are summarized in the empirical probability density function (pdf) $f(y|R)$.

The set of non-reported defects (level 1 in Figure 1) is measured and recorded by the IT, but the ILI vendor does not report them to the pipeline operator if the measured depth values fall below the reporting threshold. In principle, the number m|NR of non-reported defects and the measured depths y_i|NR < RT (i = 1 , …, m|NR) are available. The empirical pdf $f(y|NR)$ is assumed to be available for the subsequent analysis.

Level 2:

The population of reportable defects (level 2 in Figure 1) is the union of the two sets of reported and non-reported defects. Hence, the number m of reportable defects is the sum of the number of reported and non-reported defects:

$$m = m|R + m|NR \quad (1)$$

If the non-reported defects are neglected or they are not available for the population-based corrosion growth analysis, the number of

reportable defects is equal to the number of reported defects ($m = m|\mathrm{R}$).

The pdf $f(y)$ of the depth Y of all m reportable defects (level 2 in Figure 1) is a weighted combination (Hogg et al. 2005) of the pdfs $f(y|\mathrm{R})$ and $f(y|\mathrm{NR})$, which are the pdfs of the depth of reported and non-reported defects, respectively:

$$f(y) = p(\mathrm{R})\, f(y|\mathrm{R}) + p(\mathrm{NR})\, f(y|\mathrm{NR}) \qquad (2)$$

where the weights $p(\mathrm{R}) = m|\mathrm{R} / m$ and $p(\mathrm{NR}) = m|\mathrm{NR} / m$ are the ratios of reported and non-reported defects to the total number of reportable defects, respectively. In the case where the non-reported defects are excluded from the analysis, the pdfs of the reported and reportable defects sizes are equal ($f(y) = f(y|\mathrm{R})$).

Level 3:

Level 3 in Figure 1 focuses on the distinction between true and false calls. Using Bayes' Theorem (Box and Tiao 1973) the three populations of reportable defects, true calls, and false calls having pdfs $f(y|\mathrm{TC})$, $f(y|\mathrm{FC})$, and $f(y)$, respectively, are related as follows (Pandey 1998):

$$f(y|\mathrm{TC}) \sim \mathrm{POTC}(y)\, f(y) \qquad (3)$$

$$f(y|\mathrm{FC}) \sim \{1 - \mathrm{POTC}(y)\}\, f(y) \qquad (4)$$

where "~" refers to direct proportionality and POTC(y) is the probability of a true call as a function of the defect depth y. The term 1 – POTC(y) in (4) refers to the probability of a false call. In general POTC(y) increases with increasing defect depth, but the exact shape of POTC(y) is IT-dependent. It is currently not a requirement of the ILI vendors to provide information on the POTC potential of ILI tools (POF 2009). The following relationship between y and POTC is often assumed (Maes and Salama 2008):

$$\mathrm{POTC}(y) = 1 - \exp(-y / y_T) \qquad (5)$$

where y_T is the mean credible depth. Figure 2 shows an example of a POTC curve based on (5) using y_T = 20% nwt. The corresponding probability of a false call is also given in the same figure. While POTC increases with larger depth y, the probability of a false call decreases. Figure 3 provides an example where the pdfs of the defect depth for the populations of true calls, false calls, and true and false calls (reportable defects) are compared using the POTC and POFC curves from Figure 2. The pdf of the true calls tends to preserve deeper defects due to the fact that the true call potential favors the affirmative identification of larger defects. Therefore, the likelihood that an observed defect depth y is not a false call is greater for deeper defects. The pdf of the false calls lies close to the pdf of all reportable defects due to the shift towards smaller defects and the associated high false call potential.

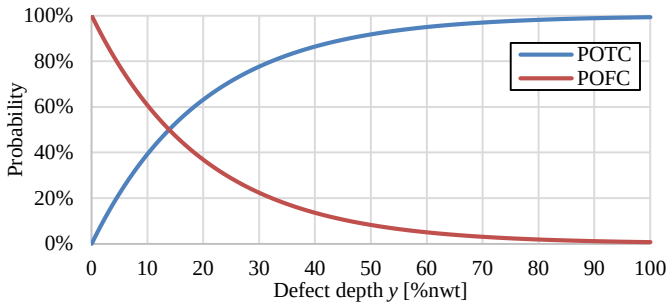

Figure 2: Examples of the probability of true call and probability of false call as a function of the defect depth.

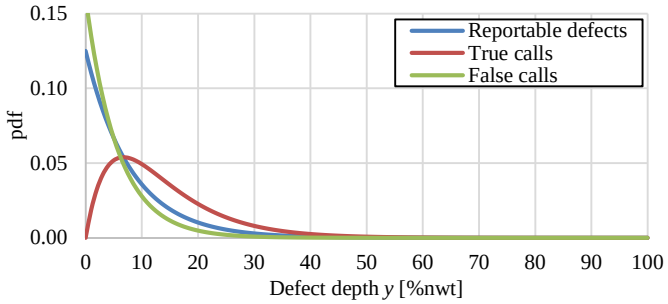

Figure 3: pdf of the defect depth for the population of true calls, false calls, and the union of the two populations (reportable defects).

The set of reportable defects divides into the sets of true and false calls at level 3 in Figure 1. The sum of the number of true calls $m|\mathrm{TC}$ and false calls $m|\mathrm{FC}$ is equal to the total number m of reportable defects:

$$m|\mathrm{TC} + m|\mathrm{FC} = m \qquad (6)$$

Point estimates for the number of true and false calls are obtained as follows:

$$\hat{m}\,|\mathrm{TC} = m\int \mathrm{POTC}(y)f(y)\mathrm{d}y \quad (7)$$

$$\hat{m}\,|\mathrm{TF} = m - \hat{m}\,|\mathrm{TC} \quad (8)$$

The variance Var[m|TC] of the number of true calls can be determined as:

$$\mathrm{Var}[m|\mathrm{TC}] = m\int \mathrm{POTC}(y)[1-\mathrm{POTC}(y)]f(y)\mathrm{d}y + m^2\{\int \mathrm{POTC}^2(y)f(y)\mathrm{d}y - [\int \mathrm{POTC}(y)f(y)\mathrm{d}y]^2\} \quad (9)$$

The variance for the number of false calls is estimated by adjusting (9) for false calls. A α%-confidence intervals can be determined for the number of true and false calls using the point estimates in (7) and (8):

$$\{\hat{m}\,|\mathrm{TC} - z_{\alpha/2}\mathrm{SD}[m|\mathrm{TC}];\ \hat{m}\,|\mathrm{TC} + z_{\alpha/2}\mathrm{SD}[m|\mathrm{TC}]\} \quad (10)$$

$$\{\hat{m}\,|\mathrm{FC} - z_{\alpha/2}\mathrm{SD}[m|\mathrm{FC}];\ \hat{m}\,|\mathrm{FC}] + z_{\alpha/2}\mathrm{SD}[m|\mathrm{FC}]\} \quad (11)$$

where $z_{\alpha/2}$ is the standard Gaussian percentile and SD[ ] indicates the standard deviation, which is obtained from the variance in (9).

Level 4:

The step from level 4 to level 3 in Figure 1 includes the sizing error. An additive sizing error model is commonly assumed for ILI data (Maes and Salama 2008):

$$y|\mathrm{TC} = a + b(x|\mathrm{TC}) + \varepsilon \quad (12)$$

where y|TC is the depth of all true calls subject to sizing error and x|TC is the actual depth of all true calls. The intercept a and the slope b are the bias and multiplier, respectively, for the actual depth; they are IT-dependent. The variable ε represents the random scatter in the depth sizing model and is assumed to be normally distributed with a mean value of zero and a known standard deviation σ_ε. Solving equation (12) for the actual size x|TC of the true calls provides the required relationship to adjust the given y|TC from level 3 in Figure 1:

$$x|\mathrm{TC} = (y|\mathrm{TC} - a - \varepsilon) / b \quad (13)$$

Based on (13), x|TC follows a normal pdf $f(x|(\mathrm{TC}, y|\mathrm{TC}))$ conditional on y|TC with a mean value of $(y|\mathrm{TC} - a) / b$ and a standard deviation of σ_ε / b. The marginal pdf $f(x|\mathrm{TC})$ is obtained by integration over the entire range of y|TC:

$$f(x|\mathrm{TC}) = \int f(x|(\mathrm{TC}, y|\mathrm{TC}))f(y|\mathrm{TC})\mathrm{d}y \quad (14)$$

Because the sizing error only affects the defect size at levels 3 and 4 in Figure 1, the number n|TC of true calls, including the confidence interval, is the same as for m|TC in (7) and (10).

Level 5:

The top level in Figure 1 contains the population of true corrosion defects in the pipeline. This set of defects divides into the population of successfully detected defects (true calls) and the population of non-detected defects. The pdfs for the defect depth of the detected and the entire set of defects are related as follows using Bayes' Theorem (Pandey 1998):

$$f(x) \sim f(x|\mathrm{TC}) / \mathrm{POD}(x) \quad (15)$$

where $f(x)$ is the pdf of the actual depth X of all detected and non-detected defects, $f(x|\mathrm{TC})$ is the pdf of the depth X|TC of all detected defects, and POD(x) is the probability of detection as a function of x. POD increases with increasing defect depth. ILI vendors typically report the required depth value where a POD of 90% is achieved (POF 2009). Because the complete POD(x) function is IT-dependent, an exponential distribution is assumed for POD(x) (Maes and Salama 2008):

$$\mathrm{POD}(x) = 1 - \exp(-x / x_D) \quad (16)$$

where x_D is the mean detection threshold. The number n of all true defects in the pipeline is the sum of the number of detected n|TC and non-detected defects n|ND:

$$n|\mathrm{TC} + n|\mathrm{ND} = n \quad (17)$$

The point estimate $\hat{n}$ and the variance Var[n] of n is inferred:

$$\hat{n} = (n|\mathrm{TC}) / \int \mathrm{POD}(x)f(x)\mathrm{d}x \quad (18)$$

$$\mathrm{Var}[n] = \hat{n}\int \mathrm{POD}(x)[1-\mathrm{POD}(x)]f(x)\mathrm{d}x + \hat{n}^2\{\int \mathrm{POD}^2(x)f(x)\mathrm{d}x - [\int \mathrm{POD}(x)f(x)\mathrm{d}x]^2\} \quad (19)$$

The α%-confidence interval for the number n of true corrosion defects in the pipeline is as follows:

$$\{\hat{n} - z_{\alpha/2}\mathrm{SD}[n];\ \hat{n} + z_{\alpha/2}\mathrm{SD}[n]\} \quad (20)$$

where $z_{\alpha/2}$ is the standard Gaussian percentile and SD[n] is the standard deviation of n. Although not relevant for the integrity assessment of pipelines, the pdf $f(x|\mathrm{ND})$ of the size and the number $n|\mathrm{ND}$ of non-detected defects (level 4 in Figure 1) can be estimated:

$$f(x|\mathrm{ND}) \sim (1 - \mathrm{POD}(x))\, f(x) \quad (21)$$

$$\hat{n}|\mathrm{ND} = \hat{n} - \hat{n}|\mathrm{TC} \quad (22)$$

where $\hat{n}|\mathrm{TC} = \hat{m}|\mathrm{TC}$. The term 1 – POD($x$) in (21) represents the probability of non-detection. Figure 4 shows an example of a POD curve using a mean detection threshold of x_D = 10% nwt. The probability of non-detection is also given.

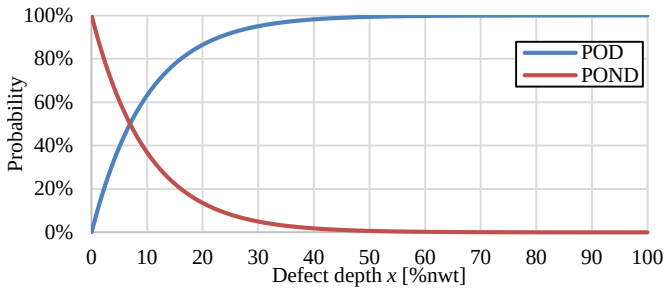

Figure 4: Examples of probability of detection and probability of non-detection as a function of the actual defect depth.

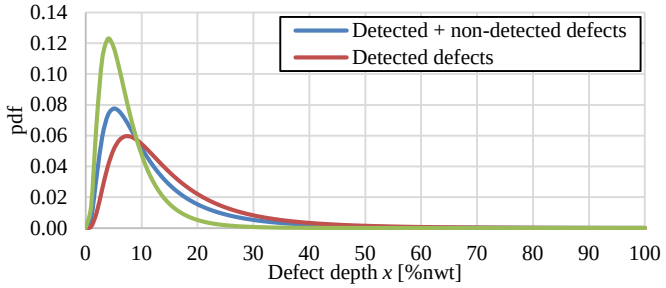

Figure 5: pdf of defect depth for the population of detected defects, non-detected defects, and the union of detected and non-detected defects.

Figure 5 compares the pdfs of the defect size for the populations of true calls, non-detected defects, and the union of the two populations. The POD curve injects many smaller defects into the population of all defects as they have a low likelihood of detection.

The analysis presented in this section allows one to determine the population of actual defects in a pipeline with respect to defect depth and the number of defects for a given individual ILI. The reported defect depths and numbers are adjusted for false calls, sizing errors, and detectability uncertainties.

4. ANALYSIS OF THE POPULATION CORROSION GROWTH BETWEEN INSPECTIONS

The corrosion growth between two ILIs can be modeled – independent of whether a matched defect pair or two populations of defects are considered – as the following sum:

$$X_2 = X_1 + \Delta X \quad (23)$$

where X_2 is the actual defect depth at the second ILI, X_1 is the actual defects depth at the first ILI, and ΔX is the corrosion growth increment ($\Delta X \geq 0$) between the two inspections. While the previous section focused on estimating the distribution of the actual defect depth X_1 and X_2 in (15), the objective in this section is to determine current and future corrosion growth. The relationship between the pdfs of X_1, X_2, and ΔX is defined by the convolution integral:

$$f_{X2}(x_2) = \int f_{X1}(x_1) f_{\Delta X}(x_2 - x_1)\mathrm{d}x_1 \quad (24)$$

where $f_{X2}(x_2)$ is the pdf of X_2, $f_{X1}(x_1)$ is the pdf of X_1, and $f_{\Delta X}(x_2 - x_1)$ is the pdf of the corrosion growth ΔX. Because the pdfs $f_{X1}(x_1)$ and $f_{X2}(x_2)$ are known (15), the objective is to determine the pdf $f_{\Delta X}(\Delta x)$. A generic, closed-form de-convolution (Meister 2009) of (24) is not available to determine $f_{\Delta X}(\Delta x)$. Based on (24), the first and second moments of the corrosion growth ΔX are determined to as follows:

$$\mathrm{E}[\Delta X] = \mathrm{E}[X_2] - \mathrm{E}[X_1] \geq 0 \quad (25)$$

$$\mathrm{Var}[\Delta X] = \mathrm{Var}[X_2] - \mathrm{Var}[X_1] > 0 \quad (26)$$

Instead of determining the de-convolution to find $f_{\Delta X}(\Delta x)$ in (24), a different approach is proposed that relies on the direct determination of the convolution in (24). The pdf of X_2 is determined

using the convolution in (24), assuming a distribution for the corrosion growth increment ΔX. The result is compared with the ILI-based pdf of X_2 obtained from (15). If the two pdfs are in satisfactory agreement, the parameter(s) for the distribution of the corrosion growth are estimated.

The gamma process is a suitable stochastic process to describe the corrosion growth in structures and pipelines (Maes et al. 2008; Maes et al. 2009; Maes et al. 2009; van Noortwijk 2009; Dann 2011). The corrosion growth increment ΔX in (23) is assumed to be gamma distributed with unknown shape and scale variables $\Delta\alpha$ and β, respectively:

$$\Delta X|\Delta\alpha, \beta = \text{gamma}(\Delta\alpha, \beta) \quad (27)$$

The shape variable $\Delta\alpha = \theta\Delta t$ is the product of the known time difference Δt in which the growth increment ΔX occurs and an unknown multiplier $\theta > 0$. The mean value and variance of ΔX are $\theta\Delta t\beta$ and $\theta\Delta t\beta^2$, respectively. Initial point estimates $\hat{\theta}$ and $\hat{\beta}$ for the two unknown variables θ and β are obtained by setting the first and second moment of (27) equal to the two moments of the determined growth increment in (25) and (26), respectively:

$$\hat{\theta} = \{\text{E}[X_2] - \text{E}[X_1]\}^2 / \{\text{Var}[X_2] - \text{Var}[X_1]\} \quad (28)$$

$$\hat{\beta} = \{\text{Var}[X_2] - \text{Var}[X_1]\} / \{\text{E}[X_2] - \text{E}[X_1]\} \quad (29)$$

A second pdf $f_2(x_2)$ is determined based on the convolution integral in (24) where $f_{X1}(x_1)$ is the pdf of the actual defect depth in (15) and $f_{\Delta X}(x_2\text{-}x_1)$ is the gamma-distributed pdf of ΔX in (27), parameterized with the point estimates obtained from (28) and (29):

$$f_2(x_2) = \int f_{X1}(x_1) f_{\Delta X}(x_2\text{-}x_1)\text{d}x_1 \quad (30)$$

The pdf $f_{X2}(x_2)$ obtained from the ILI data in (15) and the pdf $f_2(x_2)$ in (30) have the same first and second moments, but their shapes differ. If the difference is minimal, particularly in the upper tail of the two distributions, the initial point estimates of θ and β for describing the gamma-distributed corrosion growth process are accepted. If the difference between the two distributions is unacceptable, adjustments on $\hat{\theta}$ and $\hat{\beta}$ can be made to achieve a better fit. The pdf $f_F(x)$ of the depth of the entire defect population at future t_F is estimated, after determining the final estimates for the variables θ and β, as follows:

$$f_F(x) = \int f_{X2}(x_2) f_{\Delta X}(x\text{-}x_2)\text{d}x_2 \quad (31)$$

where $f_{X2}(x_2)$ is the pdf of the defect depth for the last ILI in (15) and $f_{\Delta X}(x\text{-}x_2)$ is the pdf of the gamma-distributed corrosion growth increment between the last ILI and the future time t_F.

5. NUMERICAL EXAMPLE

A pipeline is considered where two ILIs have been performed 3.5 years apart (Dann et al. 2015). The first and second inspections are referred to as ILI 1 and ILI 2, respectively. Table 1 shows the IT characteristics for the two inspections. The ITs have the same sizing accuracies and reporting thresholds. The IT at ILI 2 is more capable of detecting corrosion growth and has fewer false calls than the IT for ILI 1. The standard deviation of 7.8% nwt for the scatter in the sizing error model corresponds to a confidence interval of ±10% nwt at an 80% confidence level, which is the standard sizing accuracy of magnetic flux leakage ILI tools (POF 2009). The empirical probability mass function (pmf) of the reported depth values for ILI 1 and ILI 2 are provided in Figure 6. A clear observed depth growth between the two inspections is visible as well as the cut-off at 10% nwt due to the lower reporting threshold. The numbers of reported defects are 136 and 200 for the ILI 1 and ILI 2, respectively. The objective is to estimate the future corrosion growth in the pipeline for the integrity and remaining lifetime of the entire system.

The probabilistic analysis in Section 3 is used to determine the pdfs of the actual defect depth and the number of defects for the two inspections given the ILI tool characteristics in Table 1 and the ILI results in Figure 6. The defect depths below the reporting threshold are not considered and, therefore, all subsequent results represent only the defects above the reporting threshold. The results of these analyses are summarized for

ILI 1 and ILI 2 in Table 2 and Table 3, respectively.

Table 1: ILI tool characteristics for defect sizing, defect detection, true call potential, and reporting threshold.

ILI tool characteristics	ILI 1	ILI 2
Mean detection threshold x_D (%nwt)	10	8
Mean credible defect depth y_T (%nwt)	20	18
Intercept a in linear depth sizing model (%nwt)	0	0
Slope b in linear depth sizing model (-)	1.0	1.0
Standard deviation of depth sizing error σ_ε (%nwt)	7.8	7.8
Reporting threshold RT (%nwt)	10	10

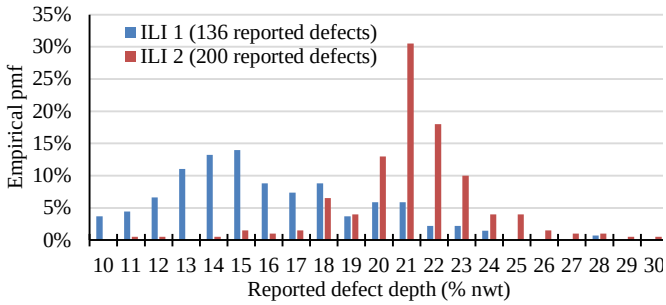

Figure 6: Two populations of reported defect depths.

Table 2: Summary of the population-based analysis for ILI 1.

	Reported defects	Actual defects
Statistics of defect depth > RT		
Mean value (% nwt)	15.9	18.0
Standard deviation (% nwt)	3.5	6.2
90th percentile (% nwt)	20	26.2
95th percentile (% nwt)	22	29.3
99th percentile (% nwt)	24	35.2
Defect count > RT		
Lower bound 95% confidence interval	---	93
Mean value	136	123
Upper bound 95% confidence interval	---	153
Most probable largest defect > RT		
Lower bound 95% confidence interval (% nwt)	---	34.9
Mean value (% nwt)	28	35.8
Upper bound 95% confidence interval (% nwt)	---	36.5

Table 2 and Table 3 compare the IT reported values with the estimates for the actual defect population. They show the summary statistics for the population depth and the number of defects. They also contain the estimated depth x_{MPL} of the most probable largest (MPL) defect. The MPL depth is the most likely largest value that would be sampled from a large population with n defects (Gumbel 1958). If the population has a pdf $f(x)$ and a cumulative distribution function (cdf) $F_X(x)$, then the estimate of x_{MPL} is as follows:

$$x_{MPL} = F_X^{-1}(1 - 1/n) \quad (32)$$

The confidence interval for x_{MPL} is determined from the upper and lower confidence bounds of n in (20). Figure 7 and Figure 8 show the pdfs of the reported defects, true calls, false calls, defects after applying the sizing error, and the actual population of corrosion defects, for ILI 1 and ILI 2, respectively. The influence of the sizing error is clearly visible in both figures as it "smoothens" the pdfs.

Table 3: Summary of the population-based analysis for ILI 2.

	Reported defects	Actual defects
Statistics of defect depth > RT		
Mean value (% nwt)	22.2	21.1
Standard deviation (% nwt)	2.6	7.1
90th percentile (% nwt)	24	30.3
95th percentile (% nwt)	25	33.3
99th percentile (% nwt)	28	39.0
Defect count > RT		
Lower bound 95% confidence interval	---	169
Mean value	200	221
Upper bound 95% confidence interval	---	274
Most probable largest defect > RT		
Lower bound 95% confidence interval (% nwt)	---	40.6
Mean value (% nwt)	30	41.4
Upper bound 95% confidence interval (% nwt)	---	42.0

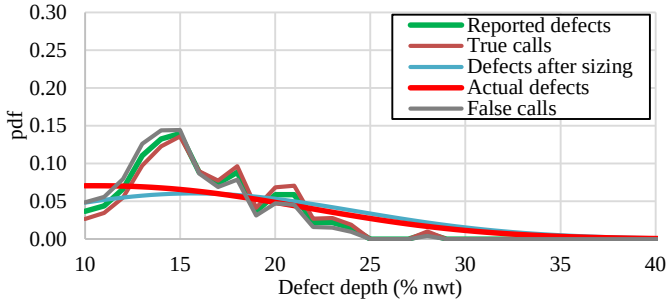

Figure 7: pdf of the defect depth for the populations at ILI 1 conditional on depth ≥ reporting threshold.

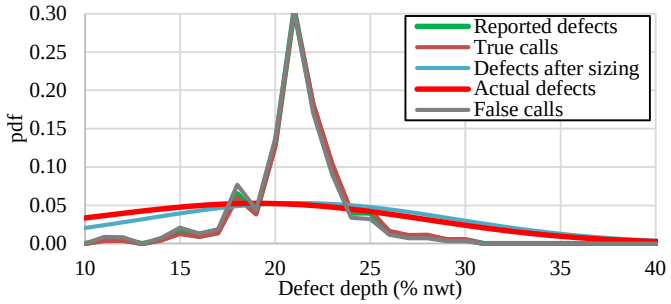

Figure 8: pdf of the defect depth for the populations at ILI 2 conditional on depth ≥ reporting threshold.

Figure 9 to Figure 12 show the pdf and exceedance probability plot for the depth of the population of actual defects for 1 to 15 years after the last inspection. The future population corrosion growth is noticeable on the shift of the pdfs towards higher depth values. The exceedance probability plots in Figure 10 and Figure 12 can be used to determine the probability $\Pr[X > x_{crit}]$ that the defect depth exceeds a given critical depth x_{crit}. For example, the critical depth for a leakage failure of pipelines is typically set to 80% nwt (ASME 2012) or 85% nwt (DNV 2010). From Figure 12, the probability that the population of actual defects exceeds the 80% nwt depth limit at 15 years after ILI 2 is 2.2×10^{-4}. An integrity and remaining lifetime assessment – either in a deterministic or probabilistic manner – can rely on the results in Figure 9 to Figure 12 to make optimal decisions with respect to inspection intervals and maintenance and repair requirements.

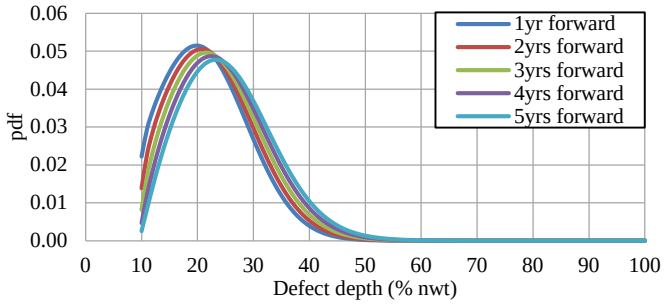

Figure 9: pdf of the estimated population depth at 1 to 5 years since the last ILI.

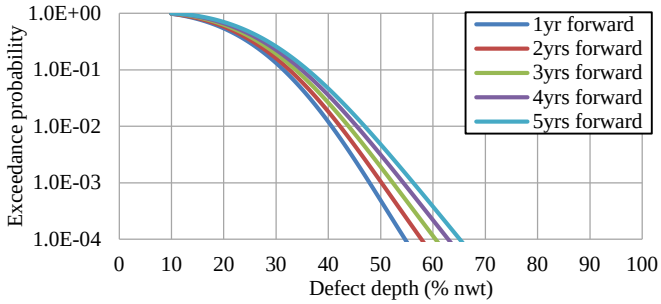

Figure 10: Log-exceedance probability plot of the estimated population depth at 1 to 5 years since the last ILI.

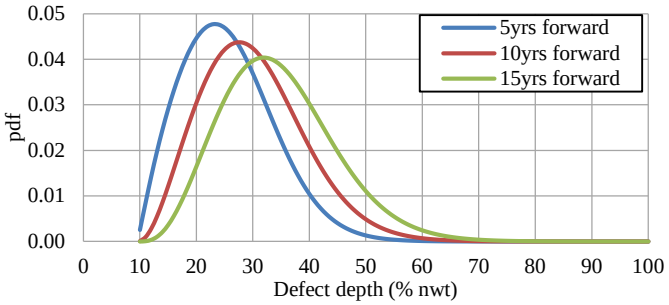

Figure 11: pdf of the estimated population depth at 5 to 15 years since the last ILI.

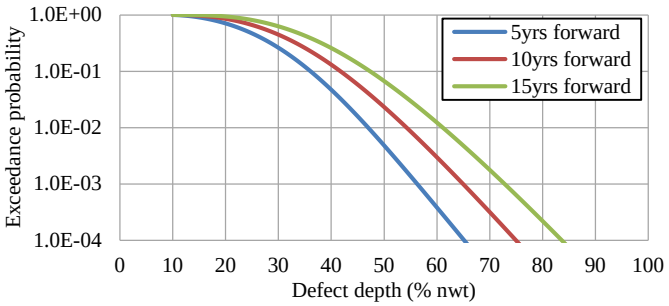

Figure 12: Log-exceedance probability plot of the estimated population depth at 5 to 15 years since the last ILI.

6. CONCLUSIONS

A new population-based framework is developed for the probabilistic analysis of ILI corrosion data. Feature matching, which is prone to uncertainties, is not required. All corrosion defects of a given inspection are considered from a group or population perspective. The probabilistic framework accounts for detectability, sizing, and false call uncertainties and relies on a stochastic growth process with strictly positive growth increments to determine the future depth of the entire population of defects in a pipeline. The analysis relies on a summary description of the number of reported defects and the pdf of the observed defects depths. Consequently, the model size remains independent of the number of reported defects. The developed analysis can be implemented in spreadsheet tools and does not require numerical simulation techniques to determine the distributions of the unknown random variables. Pipeline integrity assessments and decision making can rely on estimates of the distribution of the size of all defects in a pipeline.

ACKNOWLEDGEMENT

The support from ConocoPhillips Company is highly appreciated. The first author is also thankful for the grant from the University of Calgary.

REFERENCES

ASME (2012). Manual for Determining the Remaining Strength of Corroded Pipelines: Supplement to ASME B31 Code for Pressure Piping (ASME B31G), The American Society of Mechanical Engineers.

Box, G. E. P., and Tiao, G. C. (1973). Bayesian Inference in Statistical Analysis, Addison-Wesley Publishing Company, Reading, US.

Bubenik, T., Harper, W. V., Moreno, P., and Polasik, S. (2014). "Determining reassessment intervals from successive in-line inspections." Proc. 10th International Pipeline Conference, ASME.

Congdon, P. D. (2010). Applied Bayesian Hierarchical Methods, CRC Press, Boca Raton, US.

Dann, M. R. (2011). "Hierarchical Bayes Models in Engineering: Theory and Applications." PhD thesis, University of Calgary, Calgary, Canada.

Dann, M. R., Maes, M. A., and Salama, M. M. (2015). "Pipeline corrosion growth modeling for in-line inspection data using a population-based approach." Proc. 34th International Conference on Ocean, Offshore and Arctic Engineering, ASME.

Dawson, J. S., and Kariyawasam, S. (2009). "Understanding and accounting for pipeline corrosion growth rates." Proc. 17th Joint Technical Meeting on Pipeline Research, EPRG - PRCI - APIA.

DNV (2010). Recommended Practice DNV-RP-F101: Corroded Pipelines.

Gamerman, D., and Lopes, H. F. (2006). Markov Chain Monte Carlo: Stochastic Simulation for Bayesian Inference, CRC Press, Boca Raton, US.

Gelman, A., and Hill, J. (2007). Data Analysis Using Regression and Multilevel/Hierarchical Models, Cambridge University Press, New York, US.

Gumbel, E. J. (1958). Statistics of Extremes, Columbia University Press, New York, US.

Hogg, R. V., McKean, J. W., and Craig, A. T. (2005). Introduction to Mathematical Statistics, Pearson Prentice Hall, Upper Saddle River, US.

Maes, M. A., and Dann, M. R. (2011). "A unified probabilistic treatment for in-line inspection with respect to detectability, reportability, false call potential and depth sizing." Proc. 11th International Conference on Applications of Statistics and Probability in Civil Engineering.

Maes, M. A., Dann, M. R., and Breitung, K. W. (2009). "Reliability-based integrity assessment of structural systems subject to heterogeneous deterioration and large-scale inspection uncertainty." Proc. 10th International Conference on Structural Safety and Reliability, CRC Press.

Maes, M. A., Dann, M. R., Breitung, K. W., and Brehm, E. (2008). "Hierarchical modelling of stochastic deterioration." Proc. 6th International Probabilistic Workshop, 101-116.

Maes, M. A., Faber, M. H., and Dann, M. R. (2009). "Hierarchical Modelling of Pipeline Defect Growth subject to ILI Uncertainty." Proc. 28th International Conference on Ocean, Offshore and Arctic Engineering, ASME.

Maes, M. A., and Salama, M. M. (2008). "Managing ILI Inspection Uncertainties." PipeLine and Gas Technology, 7(5), 34-41.

Meister, A. (2009). Deconvolution Problems in Nonparametric Statistics, Springer, Berlin.

Pandey, M. D. (1998). "Probabilistic models for conditon assessment of oil and gas pipelines." NDT&E International, 31(5), 349-358.

POF (2009). "Specifications and requirements for intelligent pig inspection of pipelines." Pipeline Operators Forum.

van Noortwijk, J. M. (2009). "A survey of the application of gamma processes in maintenance." Reliability Engineering and System Safety, 94(1), 2 -21.

Zhang, S., and Zhou, W. (2014). "Bayesian dynamic linear model for growth of corrosion defects on energy pipelines." Reliability Engineering and System Safety, 128, 24-31.

Zhang, S., Zhou, W., and Qin, H. (2013). "Inverse Gaussian process-based corrosion growth model for energy pipelines considering the sizing error in inspection data." Corrosion Science, 73, 309-320.